Millimeter-wave Optical Network Analysis

Jon Martens

[Summary] The desire for higher single-wavelength modulation bandwidths in optical networks requires broader band RF characterization of components including electrical-to-optical (EO) and optical-to-electrical (OE) converters and this is often done with microwave techniques. Extending these measurements to the mm-wave regime, may require added attention to the measurement techniques, uncertainties, and characterization processes.

1 Introduction

There has been no reduction in the desire for increasing aggregate bandwidth in optical communications links. For many years, the increase was mainly accomplished by multiplexing additional optical wavelengths (or other optical parameters) or changing modulation techniques but perhaps not increasing the per-carrier modulation bandwidth. Recently, there has also been a desire to increase each of these modulation bandwidths which means increasing RF bandwidths on the electrical side of the system into the 100+ GHz range[1)-2)]. In turn, this pushes the RF characterization tools for the optical conversion and other components into the higher mm-wave regimes. This characterization may also include modulation domain measurements of purely optical components as the bandwidths can start to interact with traditionally optical mechanisms.

Measurements of optical converters to mm-wave frequencies will be explored here with a focus on changes happening at higher frequencies. Subtopics include the calibration and de-embedding steps, primary device characterization (to use as transfer standards) and composite uncertainties. Examples will be considered, and the effects of changing device media (in an RF connectivity sense) will also be presented.

2 Measurement approach

The main aim of network analysis with optical conversion components is to evaluate the 'channel' impairments that an information signal would experience during modulation and demodulation steps. Usually, this is just done with the standard swept CW tone of a vector network analyzer (VNA) but, if there are significant nonlinearities in play, an actual modulated signal could be used as well[3)].

With 100+ GHz of available modulation range in some conversion components, a broadband VNA becomes are requirement and instruments reaching to 220+ GHz are available[4)]. The broadband aspect can be important as digital signals normally form the information payload in these systems, so it is a continuous bandwidth requirement from near DC and not a banded one. Structure in the frequency response function, even at intermediate frequencies, could introduce bit error rate or eye diagram issues. Because of the importance of the response form, the calibration of the VNA can take on added importance at the higher frequencies. This can be particularly relevant when the physical media are unconventional (e.g., the modulator is excited with wafer probes, or the detector is in a microstrip fixture).

Eye diagrams are important to assessing the effect of the functional response and it is common to use the mm-wave channel data (showing loss, phase slope and structure) to compute the effect on a digital signal and this is also commonly done as part of the network analysis procedure. An example eye diagram for a 56 Gbaud/s PAM4 signal traversing a 145 GHz EO/OE path is shown in Figure 1 along with a native response without the EO/OE system. Note that the vertical scales in this figure are not the same, and net loss was not compensated. The roll-off of the optical path was not extreme to 145 GHz so the eye distortion was modest for this signal.

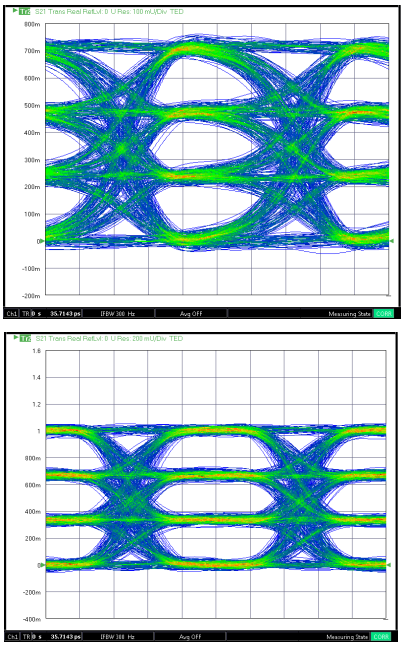

Figure 1 Eye diagrams of a 56 Gbaud/s PAM4 signal passing through an EO-fiber-OE chain (measured to 145 GHz; top) and the same signal just measured directly by the same 145 GHz receiver (bottom). There is a change of the eye shape with the optical path as the converters had loss slope with frequency. No pre-emphasis or gain correction was used for these measurements.

Typically, one wants to identify the behavior of a particular component (e.g., a modulator) and the use of characterized devices and de-embedding allows extract the response of one component from that of the chain. The conversion behavior of one device (a photodiode for the discussion here) is characterized in a traceable fashion and then this information is propagated to other devices by de-embedding from the composite measurement as suggested in Figure 2. In that figure, the base VNA calibration puts the reference planes at the RF inputs of the EO and OE devices so a S_{21} measurement gives a picture of conversion losses and the optical path between the converters. By de-embedding the now 'known' characteristics of one of the converters, the measurement reveals the characteristics of the other converter and those of the optical path[5]. Typically, only the transmission characteristics of the OE are used so the loss and phase change of that device are removed from the measurement. Since the EO-OE chain is rarely bilateral, multiple match interactions between the two ports are not a problem and more complete de-embedding methods offer little benefit.

That optical path between the converters may be negligible in a loss sense but other characteristics may be relevant as will be discussed in a later section. An additional de-embedding step can be used to reveal (a limited number of) optical path characteristics (loss and group delay) once the converters are known.

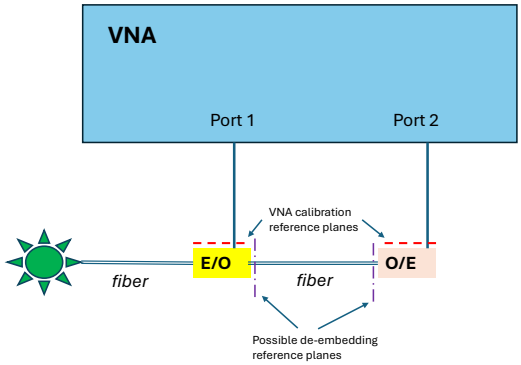

Figure 2 A typical measurement setup where an electrical VNA calibration is performed to set initial reference planes, and the de-embedding is used to remove EO and/or OE converter effects (in a conversion loss sense).

3 Characterized OE devices

A high-quality characterization of one of the conversion devices is needed to be able to solve for the other. This process can start on either side but here we use the photodetector as the basis as its stability over time is easier to quantify and the bias dependencies are often weaker. The base characterization is often done using electro-optic sampling (EOS)[6] where a very narrow optical pulse (on the femtosecond scale, compared to the expected picosecond-scale impulse response of the photodiode) is used to excite the photodiode and the photodiode's output pulse is analyzed temporally. From a transform of that output pulse, the frequency response of the photodiode is obtained. An example pulse and frequency response curve for a 145 GHz photodiode obtained with an EOS process[7] is shown in Figure 3. It is interesting to note that the frequency response curve is not entirely monotonic. Internally, the photodiode has multiple mismatch centers on the RF side (including the RF connector) and within the active region itself that can lead to minor ripple. Importantly, this frequency response structure is stable in time so the device can act as a transfer standard. Also of note is that the phase of the frequency response is also extracted, and this can be useful for evaluating group delay distortions through the path or the device of interest. The full phase function would have a steep slope corresponding to the electrical length of the device and it is deviations from a linear slope that are of primary interest and this deviation is plotted in Figure 3.

This primary electrical response can then be used to characterize a modulator or other parts of the system, through de-embedding, as was discussed in the previous section. This process can then be extended by using a now-known modulator/EO device to evaluate a new photodiode.

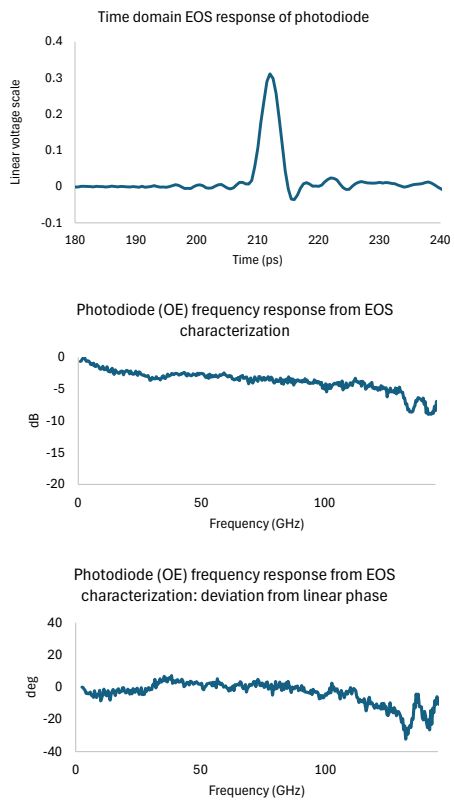

Figure 3 The EOS impulse response of an example 145 GHz photodiode is shown along with the frequency domain transformed responses (magnitude and phase).

The EOS fundamental process is extensible in bandwidth so characterizing higher frequency diodes is possible. The laser pulse widths available readily are not a limit (until at least 500 GHz). The transmission structure for temporal analysis is also readily doable to at least 220 GHz but, as this is usually done on-wafer, it does bring in additional considerations for the probe design and the calibration procedure.

4 Uncertainty topics

The measurements of any of the components in the EO-OE chain have a variety of uncertainty contributors. The most direct is the VNA measurement itself and this purely electrical measurement has been studied in the literature extensively[8)-11)]. The calibration process contributes some uncertainty and receives much attention. Since many broadband modulators and detectors have significant RF mismatch (e.g., −5 dB above 100 GHz is not uncommon as of this writing), the residual mismatch terms can be noticeable. Electrical connection repeatability and drift may be important. Network analyzer linearity can sometime play a role but typically the setup can be constructed (keeping RF signal levels bounded at certain locations) so this is of minimal importance. Since the conversion losses in many optical devices are high, one may run into signal-to-noise limits in the VNA measurement, particularly at low optical power levels. The latter follows if one looks at the modulated optical signal as in the sketch of Figure 4. If the optical power drops, the modulation sidebands will also generally drop in amplitude, and this will directly reduce the power to the VNA receivers.

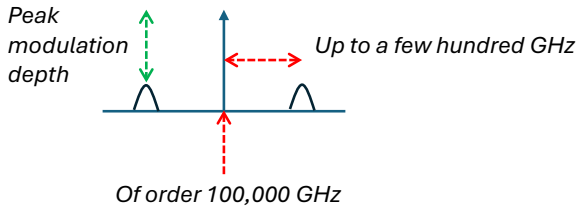

Figure 4 Spectrum of the optical signal incident on the photodiode when measuring a conventional modulator.

One can see the result of this in composite EO-OE measurements at three optical power levels as in Figure 5. Even though the curve shapes are unchanged, they get closer to the VNA noise floor (nominally −110 dB on this scale) so dB-scale impacts are possible at −25 dBm optical power in this example. Reducing the IF bandwidth of the VNA measurement, using access loops (to reduce loss to the receiver) or increasing RF power (up until linearity of the VNA or the EO system are challenged) are all means to mitigate this. Changes in the highest frequency structure are due to nonlinearities in this setup.

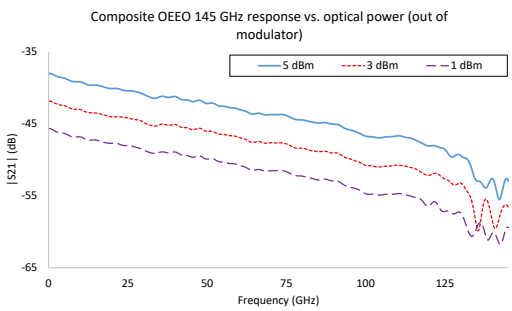

Figure 5 Optical power impacts on measured EO-OE responses.

Compared to lower frequencies (<70 GHz), the broadband

frequencies discussed do increase measurement challenges:

- A modest degradation of noise floor specifications (e.g., −100 to −110 dBm instead of −120 or −130 dBm)
- A worsening of connector repeatability and cable drift
- An increase in calibration-related uncertainties (which are compounded in mixed media scenarios to be discussed)

The optical system itself may introduce additional uncertainty terms including optical power stability, repeatability and drift of the optical connections, and bias stability (of either EO or OE components).

There is also the uncertainty in the characterization of the primary converter used for the de-embedding process (usually traceable to a National Metrology Institute). Often, this begins with the EOS process discussed in the previous section and uncertainties include residuals from mismatch correction, finite bandwidths, and imperfections in de-embedding steps[6]. An example characterization curve along with uncertainty limits is shown in Figure 6.

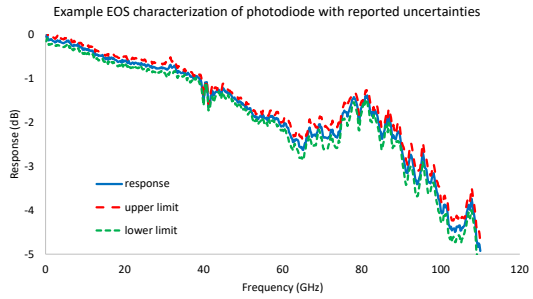

Figure 6 An example of a primary (EOS-based) characterization of an OE (photodiode) device along with the upper and lower uncertainty limits.

The combination of these uncertainties can follow one of the several established practices[8), 11)] and can lead to a better understanding of when different terms are dominant.

5 Measurement examples

A simple example would be the characterization of an EO modulator to 145 GHz. A photodiode characterized by EOS to this frequency range was available and that EOS data will be used for de-embedding. First, the VNA (Anritsu ME7838D) was calibrated using a 0.8 mm coaxial calibration kit. We would expect transmission uncertainties of 0.1-0.2 dB for higher signal levels and the noise floor of this instrument is −100 to −110 dBm over most of the frequency range[12]. The photodiode characterization uncertainties, in this case and unlike Figure 6, were highest below 30 GHz (increasing to 1 dB at the low end) and averaging 0.4 dB over the higher frequencies.

Combining these uncertainty terms, one can end up with a plot as shown in Figure 7. Because of the influence of the VNA noise floor and the dependence on optical power, the x-axis in in terms of detector signal level. For these measurement with 3 dBm optical power into the detector, and given the responsivities involved and the −10 dBm RF drive, the received level will not be below −50 dBm. At high frequencies, repeatability and VNA calibration residuals tend to dominate while, at lower frequencies, initial photodiode characterization is more important.

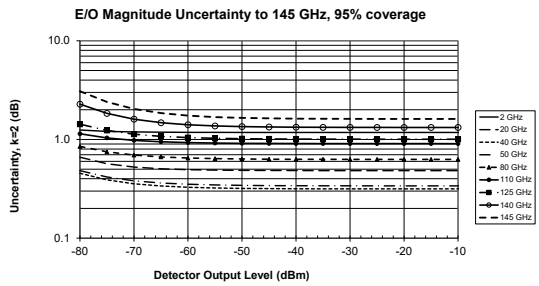

Figure 7 A calculated uncertainty curve for the extraction of an EO response to 145 GHz. This includes uncertainty terms from VNA measurement, OE characterization, aspects of the optical setup and repeatability.

The composite response and the result after de-embedding are shown in Figure 8. Both responses are normalized to 0 dB at low frequencies. In this case, the de-embedding had only modest effects below about 130 GHz indicating the EO roll-off was dominating the composite measurement. At the higher frequencies, the OE photodiode had more roll-off on its own (per the characterization), so the extracted EO response shows more of a difference. The corresponding eye (with a similar setup to Figure 1 but with a different normalization) is in Figure 9 for the EO alone. One can see an eye width reduction from that in Figure 1-lower as would be expected for such a loss profile.

At the higher data rates, there are cases where the bandwidth characteristics of the optical components can contribute[13]. One example is a polarization-maintaining fiber where the two RF modulation sidebands on the optical carrier may see different phase velocities with the difference increasing with modulation rate. When these sidebands recombine in the (nonlinear) photodetection process, the phase difference can convert to an amplitude difference. The change in dispersion of the fiber can come with a connection

process, a change in mechanical stress applied or a seemingly innocuous fiber substitution. An example is shown in Figure 10 and has the appearance of a change in RF bandwidth.

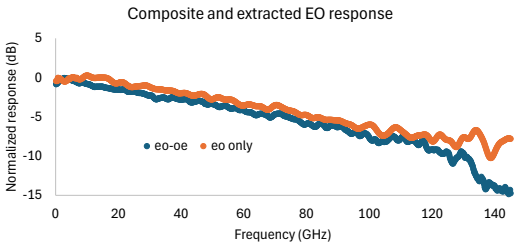

Figure 8 An example composite EO-OE response along with the de-embedded EO result to 145 GHz.

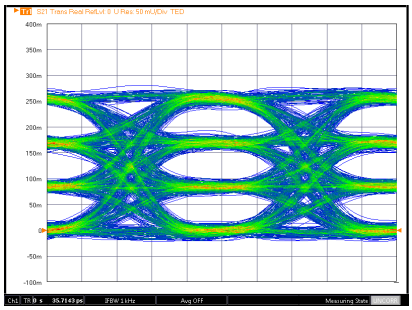

Figure 9 The computed eye diagram response for the EO of Figure 8 with a 56 Gbaud/s PAM4 signal into a 145 GHz system.

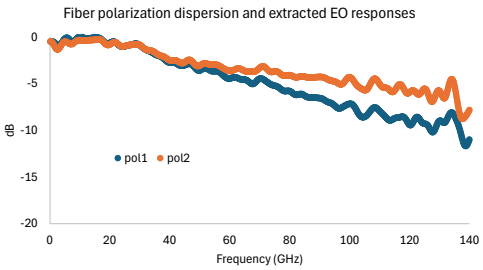

Figure 10 An example showing how a change in fiber polarization dispersion results in a perceived bandwidth change in an extracted EO device response.

6 Mixed-media complications

With higher levels of optical system integration (to include the popular area of Silicon Photonics[14]), this type of measurement more often includes mixed media (e.g., one port is probed on-wafer and another port may be fixtured or coaxial). A sketch of such a setup is in Figure 11a. Not only is the optical engineering more complex[15] but the mm-wave calibration and de-embedding is more challenging and perhaps elevates uncertainties.

There are several options on how to perform the network analysis calibration:

(1) Perform the VNA calibration on-wafer and then embed a probe's or fixture arm's characteristics (Figure 11b)

This can make use of standard on-wafer calibration methods that are relatively well-understood into the mm-wave range. There are issues (e.g., higher order mode propagation on the wafer/substrate, coupling to nearby metallized structures…)[16] but the geometry is at least controlled. Characterizing the probe/fixture arm is critical and this network extraction problem has been discussed extensively[17]. The uncertainties usually increase with frequency.

(2) Perform the VNA calibration coaxially and de-embed probes (see Figure 11c)

At modest mm-wave frequencies (e.g., to 150 GHz), this may be simpler as well-characterized coaxial calibration kits exist. The probe characterization challenge remains.

(3) Perform a hybrid calibration where two base calibrations (e.g., an on-wafer calibration and a coaxial calibration) are combined with the use of a single reciprocal device[18] (often a probe). See Figure 11d.

Here a portion of the error coefficients from two base calibrations are combined with a reciprocal processing step[18] to form the calibration at the desired reference planes. This is usually a lengthier procedure and can be mechanically complex to execute. It does avoid the need for separate probe characterization (or knowledge of the probe's characteristics from another source).

All of these approaches add to VNA uncertainties, and the ideal choice may depend on mechanical details of the setup (e.g., how difficult to demount each probe or fixture arm). Above 100 GHz, these additional steps may add a few tenths of a dB or more of net uncertainty. From an electrical point of view, the repeatability of the different connections is a factor as may be the mismatch of the EO and OE devices (i.e., for the more mismatched device, repeatability and calibration uncertainties may have greater impact so more care on that port may be warranted).

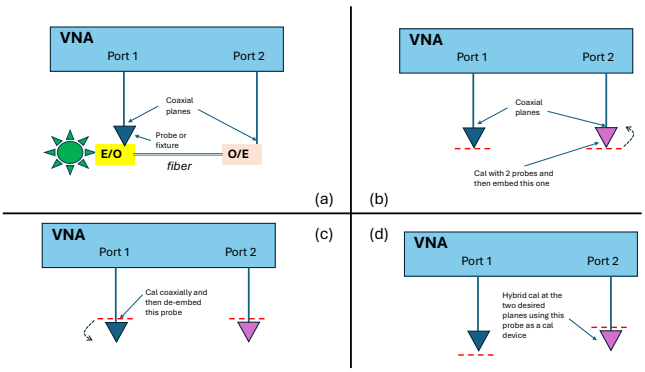

Figure 11 A situation where one optical converter uses a different RF media connection than the other (Figure 11a). There are a number of different VNA calibration approaches to handle this (Figures. 11b-d).

7 Conclusions

The desire for increasing direct modulation bandwidths on optical links has helped drive higher frequency characterization methods for optical converters (and related devices) using broadband network analyzers and broadband primary device measurements. At these higher frequencies, uncertainties increase, the dominant terms may change, and new ones may appear. As integration is also increasingly needed at these frequencies, the measurement media also change and can necessitate modified calibration and de-embedding strategies.

References

1) Y. Hinakura et al., "Silicon Photonic Crystal Modulators for High-Speed Transmission and Wavelength Division Multiplexing", *IEEE J Sel Top Quantum Electron*, vol. 27, pp. 4900108, 2020.

2) M. He et al., "High-performance hybrid silicon and lithium niobate Mach-Zehnder modulators for 100 Gbit s-1 and beyond", *Nat. Photon.*, vol. 13, pp. 359-364, 2019.

3) J. Martens, "Millimeter wave VNA characterization using modulated signals: 5G simulated modulation signal measurement to >40GHz with Vector Star and wide bandwidth high-speed digitizer," *Anritsu Tech. Review*, 2016.

4) J. Martens and T. Roberts, "Broadband 220 GHz network analysis: structures and performance," *94th ARFTG Conf. Dig.*, Jan. 2020.

5) T. Albrecht, J. Martens, T.S. Clement, P.D. Hale, and D.F. Williams, "Broadband characterization of optoelectronic components to 65 GHz using VNA techniques," *62nd ARFTG Conf. Dig.*, Dec. 2003.

6) D.F. Williams, P.D. Hale, T.S. Clement, and J.M. Morgan, "Calibrating electro-optic sampling systems, " *2001 IEEE MTT-S Int. Micr. Symp. Dig.,* June 2001.

7) P. D. Hale, et al, "Traceability of high-speed electrical waveforms at NIST, NPL, and PTB," *2012 Conf. on Precision electromagnetic Meas.*, Sept. 2012.

8) M. Wollensack, J. Hoffmann, J. Ruefenacht, and M. Zeier, "VNA Tools II: S-parameter uncertainty calculation," *79th ARFTG Conf. Dig.*, June 2012.

9) K. Wong, "Traceability of vector network analyzer measurements," *72nd ARFTG Conf. Dig.*, pp. 157-167, December 2008.

10) Guidelines on the Evaluation of Vector Network Analysers (VNA), European Association of National Metrology Institutes (EURAMET), cg-12, Version 2.0, March 2011.

11) BIPM, IEC, IFCC, ILAC, ISO, IUPAC, IUPAP and OIML, Evaluation of measurement data - Guide to the expression of uncertainty in measurement, International Organization for Standardization (ISO), September 2008 (and supplement 2).

12) Anritsu Company, "ME7838D Series Network Analyzers Technical Data Sheet," publication 11410-00778T, 2023.

13) S. Yuju, "Research on the dispersion problem in highspeed optical communication systems," *2011 2nd Int. Conf. on AI, Management Sci., and Elect. Comm. (AIMSEC)*, June 2011.

14) L. Liao, et al, "Silicon Photonics for Next-Generation Optical Connectivity," *2023 Opt. Fiber Comm. Conf. (OFC),* Mar. 2023.

15) vendors including https://www.mpi-corporation.com/ast/applications/silicon-photonics-on-wafer-test/

16) G. N. Phung, et al, "Influence of Microwave Probes on Calibrated On-Wafer Measurements," *IEEE Trans. Micr. Theory Techn.,* vol. 67, May 2019.

17) J. Martens, "Common adapter/fixture extraction techniques: sensitivities to calibration anomalies," *74th ARFTG Conf. Dig.*, Dec. 2009.

18) Anritsu Company, "VectorStar MS464xB Series Microwave Vector Network Analyzer: Calibration and Measurement Guide," publication 10410-00318AF, 2024.

Author

Jon Martens
Service Infrastructure Solutions
US Division
Test & Measurement Company

Publicly available